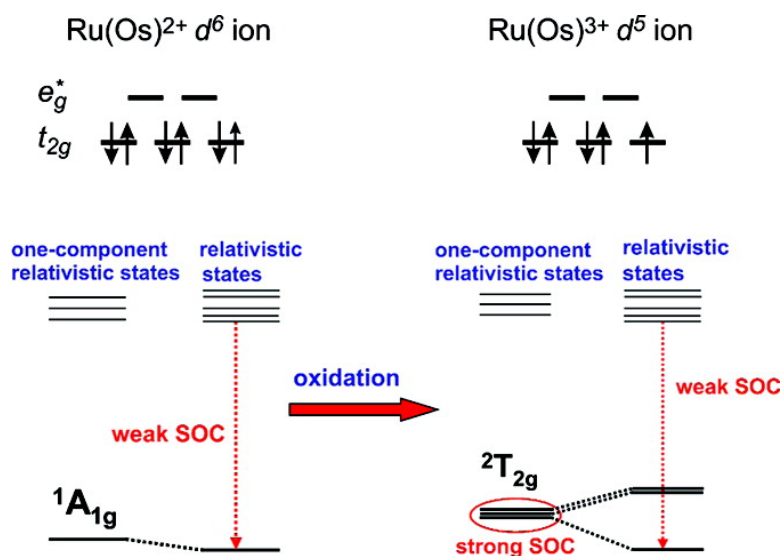Article

Effect of Spin#Orbit Coupling on Reduction Potentials of Octahedral Ruthenium(II/III) and Osmium(II/III) Complexes

Martin Srnec, Jakub Chalupsky#, Miroslav Fojta, Lucie Zendlova#, Lude#k Havran, Michal Hocek, Mojmi#r Ky#vala, and Lubomi#r Ruli#s#ek

More About This Article

Additional resources and features associated with this article are available within the HTML version:

- Supporting Information
- Access to high resolution figures
- Links to articles and content related to this article
- Copyright permission to reproduce figures and/or text from this article

View the Full Text HTML

Effect of Spin−Orbit Coupling on Reduction Potentials of Octahedral Ruthenium(II/III) and Osmium(II/III) Complexes

Martin Srnec,[†] Jakub Chalupský,[†] Miroslav Fojta,[‡] Lucie Zendlová,[†] Luděk Havran,[‡] Michal Hocek,[†] Mojmír Kývala,*[,†] and Lubomír Rulíšek*[,†]

Institute of Organic Chemistry and Biochemistry, Academy of Sciences of the Czech Republic, Centre for Complex Molecular Systems and Biomolecules, Gilead Sciences Research Center & IOCB, Flemingovo náměstí 2, 166 10 Praha 6, Czech Republic, and Institute of Biophysics, Academy of Sciences of the Czech Republic, Královopolská 135, 612 65 Brno, Czech Republic

Received January 25, 2008; E-mail: kyvala@uochb.cas.cz; lubos@uochb.cas.cz

Abstract: Reduction potentials of several $M^{2+/3+}$ (M = Ru, Os) octahedral complexes, namely, $[M(H_2O)_6]^{2+/3+}$, $[MCl_6]^{4-/3-}$, $[M(NH_3)_6]^{2+/3+}$, $[M(en)_3]^{2+/3+}$ $[M(bipy)_3]^{2+/3+}$, and $[M(CN)_6]^{4-/3-}$, were calculated using the CASSCF/CASPT2/CASSI and MRCI methods including spin−orbit coupling (SOC) by means of first-order quasi-degenerate perturbation theory. It was shown that the effect of SOC accounts for a systematic shift of approximately −70 mV in the reduction potentials of the studied ruthenium (II/III) complexes and an approximately −300 mV shift for the osmium(II/III) complexes. SOC splits the sixfold-degenerate $^2T_{2g}$ ground electronic state (in ideal octahedral symmetry) of the M^{3+} ions into the $E_{(5/2)g}$ Kramers doublet and $G_{(3/2)g}$ quartet, which were calculated to split by $1354-1573$ cm^{-1} in the Ru^{3+} complexes and $4155-5061$ cm^{-1} in the Os^{3+} complexes. It was demonstrated that this splitting represents the main contribution to the stabilization of the M^{3+} ground state with respect to the closed-shell $^1A_{1g}$ ground state in M^{2+} systems. Moreover, it was shown that the accuracy of the calculated reduction potentials depends on the calculated solvation energies of both the oxidized and reduced forms. For smaller ligands, it involves explicit inclusion of the second solvation sphere into the calculations, whereas implicit solvation models yield results of sufficient accuracy for complexes with larger ligands. In such cases (e.g., $[M(bipy)_3]^{2+/3+}$ and its derivatives), very good agreement between the calculated (SOC-corrected) values of the reduction potentials and the available experimental values was obtained. These results led us to the conclusion that especially for Os$^{2+/3+}$ complexes, inclusion of SOC is necessary to avoid systematic errors of ∼300 mV in the calculated reduction potentials.

Introduction

Quantum-chemical calculations of reduction potentials of transition-metal compounds require accurate predictions of both the enthalpic and entropic terms in the free energy difference ($\Delta G_{ox/red}$) between the oxidized and reduced forms.[1] The entropic terms can be predicted by calculating the corresponding partition functions in the ideal-gas approximation, whereas the solvation free energies are often calculated using implicit solvation models implemented in popular quantum-chemical programs.[2] The accuracy of the calculated enthalpic terms mostly depends on the approximations adopted in the electronic structure calculations.[3] Fairly accurate predictions of the reduction potentials (E^0) for species consisting of second- and third-row atoms of the main groups have been obtained using nonrelativistic calculations.[4] However, an extensive part of electrochemistry concerns transition-metal compounds possess-

ing unpaired d electrons, and hence, spin-dependent relativistic effects can significantly contribute to their ground-state energies, especially for metals in the second and third transition-metal periods. Spin−orbit coupling (SOC) is the most important of these effects. It clearly dominates the zero-field splitting (ZFS) of spin-degenerate nonrelativistic electronic states (except for spatially nondegenerate doublets) of most transition-metal-containing molecules. According to Kramers' theorem, spatially nondegenerate doublets do not split in the absence of an external magnetic field.[5] Although the electronic structures and reactivities of second- and third-row transition-metal compounds have been extensively studied (for a review, see ref 6 and references therein), SOC effects have not always been taken into account. This is the case for several studies dealing with calculations of the reduction potentials of solvated transition-

---

[†] Institute of Organic Chemistry and Biochemistry.
[‡] Institute of Biophysics.

(1) Schmidt am Bush, M.; Knapp, E. W. *J. Am. Chem. Soc.* **2005**, *127*, 15730–15737.
(2) Kettle, L. J.; Bates, S. P.; Mount, A. R. *Phys. Chem. Chem. Phys.* **2000**, *2*, 195–201.
(3) Patterson, E. V.; Cramer, C. J.; Truhlar, D. G. *J. Am. Chem. Soc.* **2001**, *123*, 2025–2031.
(4) Uudsemaa, M.; Tamm, T. *J. Phys. Chem. A* **2003**, *107*, 9997–10003.

(5) Kramers, H. A. *Proc. Acad. Sci. Amsterdam* **1930**, *33*, 959.
(6) Neese, F.; Petrenko, T.; Ganyushin, D.; Olbrich, G. *Coord. Chem. Rev.* **2007**, *251*, 288–327.
(7) Li, J.; Fisher, C. L.; Chen, J. L.; Bashford, D.; Noodleman, L. *Inorg. Chem.* **1996**, *35*, 4694–4702.
(8) Baik, M.-H.; Friesner, R. A. *J. Phys. Chem. A* **2002**, *106*, 7407–7412.
(9) Moens, J.; Roos, G.; Jaque, P.; De Proft, F.; Geerlings, P. *Chem.—Eur. J.* **2007**, *13*, 9331–9343.
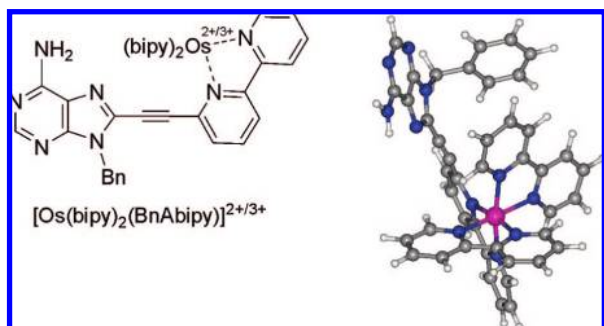(10) Rulíšek, L.; Havlas, Z. *J. Chem. Phys.* **2000**, *112*, 149–157.

Figure 1. Chemical formula and equilibrium structure of the [Os(bipy)₂(Bn-Abipy)]²⁺/³⁺ complexes as obtained from the DFT/def2-SVP (including an ECP for Os) geometry optimization. The Os−N distances are 2.07−2.11 Å for Os²⁺ and 2.07−2.13 Å for Os³⁺.

metal ions[7–9] or the spectroscopic properties of octahedral transition-metal complexes.[10,11]

Recently, there has been a growing interest in lanthanide and actinide compounds,[12–14] whose chemical behavior is dramatically influenced by SOC.[15] For example, it has been shown that the SOC contribution to gas-phase reaction energies is 0.2% for the Fe^{2+}/Fe^{3+} system,[15] whereas SOC accounts for ~36% for the UO_2^{2+}/UO_2^{+} system and markedly influences the corresponding Gibbs free energy.

In our previous work, values of the reduction potentials of a series of [Ru(bipy)₂X]²⁺/³⁺ complexes (where X stands for an ethynyl-, 4-boronophenyl-, [(9-benzyladenine-8-yl)ethynyl]-, or [4-(9-benzyladenine-8-yl)phenyl]bipyridine or phenanthroline) were calculated and compared to the corresponding experimental values.[16] Very good agreement between experiment and theory (a standard deviation of 0.13 V) was obtained. Theoretical calculations thus have predictive power for new Ru(II) complexes, though it might be difficult to reproduce differences smaller than 0.05 V. This is an important finding, since these complexes represent model compounds for electrochemical DNA labeling.[17,18] Quantum-chemical calculations can therefore assist in the search for new types of complexes with tailor-made reduction potentials.

However, the agreement was significantly poorer for the [Os(bipy)₂(BnAbipy)]²⁺/³⁺ (BnAbipy = [(9-benzyladenine-8-yl)ethynyl]bipyridine) redox pair (Figure 1), whose calculated reduction potential deviated by +427 mV from the experimental value. Qualitative considerations led us to the hypothesis that the discrepancy was caused by neglecting SOC among the three near-degenerate Kramers doublets (or, in ideal octahedral symmetry, by ZFS of the $^2T_{2g}$ ground state) of the Os³⁺ complex. Since the singlet ground state ($^1A_{1g}$) of the Os²⁺ complex is not affected at all in the zero-order model defined by neglecting all but the near-degenerate states, the extra

stabilization of the oxidized form compared to the reduced form should give rise to a negative shift of the reduction potential.

Therefore, the aim of this study was a rigorous quantum-chemical treatment of both the Ru²⁺/³⁺ and Os²⁺/³⁺ complexes. Accurate calculations must allow for relativistic effects, most importantly for SOC, which is not included in the standard density functional theory/effective core potential (DFT/ECP) model. Five types of complexes were studied, covering the most prototypical M²⁺/³⁺ (M = Ru, Os) systems: (i) hexahydrates of M²⁺/³⁺ as the reference states; (ii) small models of [M(bipy)₃]²⁺/³⁺, i.e., [M(NH₃)₆]²⁺/³⁺ and [M(en)₃]²⁺/³⁺; (iii) [M(bipy)₃]²⁺/³⁺; (iv) [MCl₆]⁴⁻/³⁻; and (v) [M(CN)₆]⁴⁻/³⁻. CASSCF/CASPT2/CASSI- and MRCI-based first-order quasi-degenerate perturbation theory (QDPT), which includes both SOC effects and the multireference character of the wave function, was used.

Computational Methods

Multireference CASSCF/CASPT2/CASSI Calculations. The complete active space self-consistent field (CASSCF),[19] complete active space second-order perturbation theory (CASPT2),[20] and multistate CASPT2 (MS-CASPT2) calculations were carried out using the MOLCAS 7.0 program.[21] For all of the atoms, the ANO-RCC basis set (contracted to [8s7p5d3f2g] for Os, [7s6p4d2f1g] for Ru, [3s2p1d] for C, N, and O, and [2s1p] for H) was used.[22] The second-order Douglas−Kroll−Hess (DKH2) one-electron spinless Hamiltonian was applied for all of the calculations in order to allow for spin-free (one-component) relativistic effects.[23–25] To address the basis-set effects, Table S1 in the Supporting Information provides a comparison of various schemes for contraction of the ANO-RCC basis set, which demonstrates that the basis set used (which is essentially TZP for metals and DZP for other elements, denoted as TZP/DZP) yielded converged results. In fact, reasonably accurate results were obtained using only the DZP contraction (see Table S1).

The computational protocol consisted of several steps: (i) geometry optimization using the DFT approach and a small basis set (the RI-J PBE/def2-SVP level, as described in DFT/ECP Calculations, below); (ii) calculation of single-point energies of the oxidized complexes using the CASSCF method with the five-electrons-in-three-orbitals [(5,3)] active space that defines our zero-order (crystal-field) model;[26] (iii) calculation of SOC among all of the states calculated in step (ii), using the complete active space state interaction (CASSI) method and solving the generalized

(11) Gilson, H. S. R.; Krauss, M. *J. Phys. Chem. A* **1998**, *102*, 6525–6532.
(12) Roos, B. O.; Malmqvist, P.-Å. *Phys. Chem. Chem. Phys.* **2004**, *6*, 2919–2927.
(13) Gagliardi, L.; Roos, B. O. *Nature* **2005**, *433*, 848–851.
(14) Roos, B. O.; Malmqvist, P.-Å.; Gagliardi, L. *J. Am. Chem. Soc.* **2006**, *128*, 17000–17006.
(15) Tsushima, S.; Wahlgren, U.; Grenthe, I. *J. Phys. Chem. A* **2006**, *110*, 9175–9182.
(16) Vrábel, M.; Hocek, M.; Havran, L.; Fojta, M.; Votruba, I.; Klepetářová, B.; Pohl, R.; Rulíšek, L.; Zendlová, L.; Hobza, P.; Shih, I.; Mabery, E.; Mackman, R. *Eur. J. Inorg. Chem.* **2007**, 1752–1769.
(17) Elias, B.; Kirsch-De Mesmaeker, A. *Coord. Chem. Rev.* **2006**, *250*, 1627–1641.
(18) Xu, L.-C.; Shi, S.; Li, J.; Liao, S.-Y.; Zheng, K.-C.; Ji, L.-N. *Dalton Trans.* **2008**, 291–301.

(19) Roos, B. O.; Taylor, P. R. *Chem. Phys.* **1980**, *48*, 157–173.
(20) Andersson, K.; Malmqvist, P.-Å.; Roos, B. O. *J. Chem. Phys.* **1992**, *96*, 1218–1226.
(21) Karlström, G.; Lindh, R.; Malmqvist, P.-Å.; Roos, B. O.; Ryde, U.; Veryazov, V.; Widmark, P.-O.; Cossi, M.; Schimmelpfennig, B.; Neogrady, P.; Seijo, L. *Comput. Mater. Sci.* **2003**, *28*, 222–239.
(22) (a) Roos, B. O.; Lindh, R.; Malmqvist, P.-Å.; Veryazov, V.; Widmark, P.-O. *J. Phys. Chem. A* **2005**, *109*, 6575–6579. (b) Widmark, P.-O.; Malmqvist, P.-Å.; Roos, B. O *Theor. Chim. Acta* **1990**, *77*, 291–306.
(23) Douglas, M.; Kroll, N. M. *Ann. Phys. (N.Y.)* **1974**, *82*, 89–155.
(24) Hess, B. A. *Phys. Rev. A* **1986**, *33*, 3742–3748.
(25) Jansen, G.; Hess, B. A. *Phys. Rev. A* **1989**, *39*, 6016–6017.
(26) The choice of the minimum active space was fairly straightforward once we realized that all of the studied complexes have well-defined low-spin ground states (either doublets or singlets) with five or six valence d electrons in the three metal t₂g MOs and that the two metal eg* MOs typically do not represent the lowest unoccupied MOs for complexes of second-and third-row transition metals. By adding the two metal eg* MOs to the minimum active space, we would allow for the effect of the (t₂g)ⁿ⁻ᵏ(eg)ᵏ configurations (k = 1–4, n = 5 or 6) on the electronic energies and wave functions of the three lowest-energy doublets while ignoring the effect of more-favorable configurations resulting from the distribution of some of the d electrons into the low-lying ligand MOs. Even if the complexes have no symmetry, the minimum active space ensures that the three near-degenerate highest occupied MOs emerge as suitable linear combinations of the five metal d atomic orbitals from the CASSCF optimization.

eigenvalue problem of first-order QDPT [taking the atomic mean-field integral (AMFI) spin−orbit Hamiltonian[27,28] as the perturbation] to obtain the SOC-corrected quasi-relativistic energies.[29] To improve the accuracy of the calculations, the CASPT2 energies were used on the main diagonal of the two-component Hamiltonian matrix.

In all of the CASSCF calculations, a level shift of 0.1 au was used in order to improve convergence. In the CASPT2 calculations, none of the orbitals were frozen, and an imaginary level shift of 0.1 au was used to eliminate intruder states.[30]

MRCI Calculations. The multireference configuration interaction (MRCI) calculations with a posteriori selection of configurations[31−34] and the CASSCF calculations used for generating input molecular orbitals (MOs) for the subsequent MRCI calculations were carried out using the ORCA 2.6.35 program.[35] These calculations used the TZV-DKH basis set, which is based on Ahlrichs' TZVP basis set (contracted to [17s11p8d3f] for Os, [12s10p5d] for Ru, [8s4p1d] for Cl, [6s3p1d] for N, O, and C, and [3s1p] for H)[36] and contracted for relativistic calculations by Neese.[35] Spin-free relativistic effects were included in all of the calculations through the DKH2 Hamiltonian.

The MRCI calculations were performed in several steps using the DFT/ECP equilibrium geometries [see also step (i) in the previous section]: (i) state-specific CASSCF calculations with a (6,5) active space for the singlet ground state of the M^{2+} complexes and state-averaged CASSCF(5,5) calculations for the three lowest doublets of the M^{3+} complexes, carried out to generate the input MOs for MRCI; (ii) calculations of MRCI-SD wave functions and energies for the three lowest-energy doublets originating in the degenerate $^2T_{2g}$ state (in ideal O_h symmetry) and of the stabilization of the lowest-energy doublet due to SOC by means of first-order QDPT; (iii) calculations of the energy stabilizations of the singlet and doublet ground states of the M^{2+} and M^{3+} complexes, respectively, due to SOC with higher states of appropriate spin multiplicities (up to quintets for M^{2+} and sextets for M^{3+}) by means of first-order QDPT.

Thresholds for configuration selection of 10^{-5} au for the reference CI space [(6,5) and (5,5) for the M^{2+} and M^{3+} complexes, respectively) and of 10^{-6} au for the CI-SD space were used, which presumably should be a good approximation to the so-called second-order CI (MRCI-SD with a CAS reference space without a posteriori selection of configuration). Orbital windows of −3 to 3 au for the Ru complexes and −1.9 to 2 au for the Os complexes were used in the MRCI calculations. The exact mean-field spin−orbit Hamiltonian was used.[27] The reason that we used the larger active spaces [(6,5) and (5,5)] as reference spaces in MRCI is that the MOs are not relaxed in the course of the MRCI calculation, and therefore, it is safer to include all five metal d-like MOs in the reference active space for nonsymmetric complexes in order to prevent errors arising from an inappropriate choice of the MO basis.

DFT/ECP Calculations. All of the DFT calculations reported in this study were carried out using the Turbomole 5.8 program.[37] The Perdew−Burke−Ernzerhof (PBE)[38] and hybrid three-parameter Becke's (B3LYP)[39] functionals were used throughout. The calculations were expedited by expanding the Coulomb integrals in an auxiliary basis set [the resolution-of-identity (RI-J) approximation].[40,41] All of the geometry optimizations were carried out using the def2-SVP basis set,[36] whereas the single-point energies were recomputed in the def2-TZVP basis set (triple-ζ valence with two polarization functions on each atom).

To allow for solvation effects, the conductor-like screening model (COSMO) method[42,43] was used with a dielectric constant corresponding to that of water ($\varepsilon_r = 80$) or of an equimolar mixture of water and acetonitrile ($\varepsilon_r = 57$) in the case of the [Ru(bipy)$_3$]$^{2+/3+}$ and [Os(bipy)$_2$L]$^{2+/3+}$ complex. The Gibbs free energy was then calculated as the sum of four contributions:

$$G = E_{el} + G_{solv} + E_{ZPE} - RT \ln(q_{trans}q_{rot}q_{vib}) \tag{1}$$

where E_{el} is the in vacuo energy of the system (at the B3LYP/def2-TZVP//RI-PBE/def2-SVP level), G_{solv} is the solvation free energy (at the RI-PBE/def2-SVP level), E_{ZPE} is the zero-point energy, and $-RT \ln(q_{trans}q_{rot}q_{vib})$ accounts for the entropic terms and the thermal correction to the enthalpy obtained from a frequency calculation using the same method and software as for the geometry optimization [at the RI-PBE/def2-SV(P) level, 298 K, and 1 atm using the ideal-gas approximation].[44]

The reduction potentials (in V) were then calculated according to the equation:

$$E^0 = 27.21(G_{ox} - G_{red}) - 4.34 \text{ V} \tag{2}$$

where G_{ox} and G_{red} are the free energies (in au) of the oxidized and reduced forms, respectively, calculated according to eq 1 and 4.34 V is the absolute redox potential of the standard hydrogen electrode.[45]

Results and Discussion

To achieve the above goal, several types of calculations were carried out. First, we demonstrated that DFT/ECP calculations yield reasonably accurate reduction potentials for Ru(II/III) complexes once solvation effects are addressed appropriately (which may involve inclusion of the second solvation shell into the calculations), whereas a systematic shift of reduction potentials occurs for Os(II/III) complexes. Next, model structures of the [M(CN)$_6$]$^{3-}$, [MCl$_6$]$^{3-}$, and [M(H$_2$O)$_6$]$^{3+}$ complexes attaining O_h or T_h symmetries were studied in order to demonstrate the SOC effects on their lowest electronic states ($^2T_{2g}$ or ^2T_g). Third, analogous results for the Jahn−Teller-distorted complexes (i.e., all of the studied systems attaining

(27) Hess, B. A.; Marian, C. M.; Wahlgren, U.; Gropen, O. *Chem. Phys. Lett.* **1996**, *251*, 365–371.

(28) Schimmelpfenning, B. AMFI Program; University of Stockholm: Stockholm, 1996.

(29) Malmqvist, P.-Å.; Roos, B. O.; Schimmelpfennig, B. *Chem. Phys. Lett.* **2002**, *357*, 230–240.

(30) (a) Roos, B. O.; Andersson, K. *Chem. Phys. Lett.* **1995**, *245*, 215–243. (b) Forsberg, N.; Malmqvist, P.-Å. *Chem. Phys. Lett.* **1997**, *274*, 196–204.

(31) Buenker, R. J.; Peyerimhoff, S. D. *Theor. Chim. Acta* **1974**, *35*, 33–58.

(32) Buenker, R. J.; Peyerimhoff, S. D. *Theor. Chim. Acta* **1975**, *39*, 217–228.

(33) Buenker, R. J.; Krebs, S. In *Recent Advances in Multireference Methods*; Hirao, K., Ed.; World Scientific: Singapore, 1999; p 1.

(34) Neese, F. *J. Chem. Phys.* **2003**, *119*, 9428–9443.

(35) Neese, F. ORCA: An ab Initio, DFT, and Semiempirical SCF-MO Package; University of Bonn: Bonn, Germany, 2007.

(36) (a) Schäfer, A.; Horn, H.; Ahlrichs, R. *J. Chem. Phys.* **1992**, *97*, 2571–2577. (b) Weigend, F.; Ahlrichs, R. *Phys. Chem. Chem. Phys.* **2006**, *7*, 3297–3305.

(37) Ahlrichs, R.; Bär, M.; Häser, M.; Horn, H.; Kölmel, C. *Chem. Phys. Lett.* **1989**, *162*, 165–169.

(38) Perdew, J. P.; Burke, K.; Ernzerhof, M. *Phys. Rev. Lett.* **1996**, *77*, 3865–3868.

(39) (a) Becke, A. D. *Phys. Rev. A* **1988**, *38*, 3098–3100. (b) Lee, C. T.; Yang, W. T.; Parr, R. G. *Phys. Rev. B* **1988**, *37*, 785–789. (c) Becke, A. D. *J. Chem. Phys.* **1993**, *98*, 5648–5652. (d) Stephens, P. J.; Devlin, F. J.; Chabalowski, C. F.; Frisch, M. J. *J. Phys. Chem.* **1994**, *98*, 11623–11627.

(40) Eichkorn, K.; Treutler, O.; Öhm, H.; Häser, M.; Ahlrichs, R. *Chem. Phys. Lett.* **1995**, *240*, 283–290.

(41) Eichkorn, K.; Weigen, F.; Treutler, O.; Ahlrichs, R. *Theor. Chim. Acta* **1997**, *97*, 119–124.

(42) Klamt, A.; Schuurmann, G. *J. Chem. Soc., Perkin Trans.* **1993**, *2*, 799–805.

(43) Schäfer, A.; Klamt, A.; Sattel, D.; Lohrenz, J. C. W.; Eckert, F. *Phys. Chem. Chem. Phys.* **2000**, *2*, 2187–2193.

(44) Jensen, F. *Introduction to Computational Chemistry*; Wiley: New York, 1999.

(45) Llano, J.; Ericsson, L. A. *Phys. Chem. Chem. Phys.* **2004**, *6*, 4707–4713.

Scheme 1. Thermodynamic Cycle Used for the Calculation of ΔG_{ox}, the Gibbs Free Energy Corresponding to the Oxidation of an $[M^{2+}X_6]$ Complex, in an Equimolar Mixture of Water and Acetonitrile ($\varepsilon_r = 57$) or in Pure Water ($\varepsilon_r = 80$)[a]
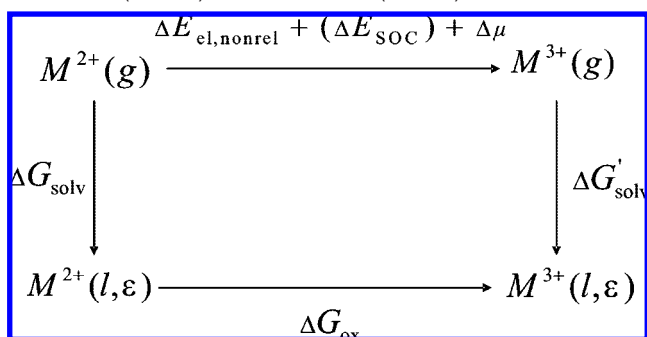
[a] The difference between the electronic energies, $\Delta E_{el,nonrel} + \Delta E_{SOC}$, along with the enthalpic and entropic corrections included in $\Delta\mu$ [$\Delta\mu = E_{ZPE} - RT \ln(q_{trans}q_{rot}q_{vib})$] determines the gas-phase free energy of the oxidation. The solvation free energies ΔG_{solv} and $\Delta G_{solv}'$ are taken into account via the implicit-solvent COSMO method.

Table 1. Reduction Potentials E^0 (V) for $[M^{2+}X_6]/[M^{3+}X_6]$ Couples, Calculated According to the Thermodynamic Cycle Shown in Scheme 1, along with Individual Energetic Contributions (eV) to the Gibbs Free Energy Corresponding to the Oxidation of M^{2+} [a]

complex	ΔE_{el}	$\Delta\Delta G_{solv}$	$\Delta\mu$	E^0(calc)	E^0(exp)
$[Ru(H_2O)_6]^{2+/3+}$	15.76	−10.02	−0.16	1.231	0.230[b]
$[Ru(H_2O)_6]^{2+/3+}\cdot(H_2O)_{12}$	11.20	−6.41	0.02	0.466	0.230
$[RuCl_6]^{4-/3-}$	−9.37	12.63	0.21	−0.863	
$[Ru(NH_3)_6]^{2+/3+}$	14.56	−9.83	0.08	0.470	0.100[b]
$[Ru(NH_3)_6]^{2+/3+}\cdot(H_2O)_{14}$	10.26	−6.35	0.35	−0.088	0.100
$[Ru(en)_3]^{2+/3+}$	13.66	−8.87	0.01	0.456	0.210[b]
$[Ru(bipy)_3]^{2+/3+}$	11.95	−6.32	−0.01	1.282	1.302,[c] 1.24[b]
$[Ru(bipy)_3]^{2+/3+}\cdot(H_2O)_{27}$	9.69	−4.31	0.17	1.219	1.302, 1.24
$[Ru(CN)_6]^{4-/3-}$	−7.56	12.30	−0.05	0.342	0.860[b]
$[Os(H_2O)_6]^{2+/3+}$	14.95	−9.96	−0.19	0.460	
$[OsCl_6]^{4-/3-}$	−10.04	12.60	0.23	−1.550	
$[Os(NH_3)_6]^{2+/3+}$	14.00	−9.80	0.01	−0.132	
$[Os(en)_3]^{2+/3+}$	13.16	−8.84	0.02	−0.003	
$[Os(bipy)_3]^{2+/3+}$	11.72	−6.38	0.01	1.005	0.80[b]
$[Os(bipy)_2L]^{2+/3+}$	11.15	−5.32	−0.07	1.424[c]	0.997[c,d]
$[Os(CN)_6]^{4-/3-}$	−7.68	12.26	−0.05	0.190	

[a] The electronic energies, ΔE_{el}, were calculated at the B3LYP/def2-TZVP level, and $\Delta\Delta G_{solv}$ ($=\Delta G_{solv}' - \Delta G_{solv}$) and $\Delta\mu$ were obtained at the RI-PBE/def2-SVP level. The $[RuX_n]^{2+/3+}\cdot(H_2O)_k$ notation stands for the $[RuX_n]^{2+/3+}$ complex with k water molecules in the second solvation shell. [b] From ref 46 ($\varepsilon_r = 80$). [c] From ref 16 [an equimolar mixture of water and acetonitrile ($\varepsilon_r = 57$) was used in order to reproduce the experimental conditions]. [d] L = BnAbipy; see Figure 1.

their C_1 equilibrium geometries) were obtained. Finally, to provide a proof of the principle, the results of the MRCI-based first-order QDPT calculations on model $[M(NH_3)_6]^{2+/3+}$, $[M(CN)_6]^{4-/3-}$, and $[M(H_2O)_6]^{2+/3+}$ complexes were compiled to demonstrate the effect of higher excited states on the energy of the ground state (singlet for Ru^{2+}/Os^{2+} and doublet for Ru^{3+}/Os^{3+}).

DFT/ECP Calculations of the $Ru^{2+/3+}$ and $Os^{2+/3+}$ Reduction Potentials. The Gibbs free energies corresponding to the process of oxidation have been calculated as depicted in Scheme 1. The results of the DFT/ECP calculations, including the individual terms contributing to the value of ΔG_{ox}, are presented in Table 1.

The electronic energy differences between the oxidized and reduced forms, ΔE_{el}, and the differences in the solvation Gibbs free energies, $\Delta\Delta G_{solv}$, are the largest terms, and they partially compensate for each other, as expected for ionization and

solvation energies of charged species. The differences in rotational−vibrational Gibbs free energies, $\Delta\mu$, are much smaller ($|\Delta\mu| \approx 0.01-0.23$ eV).

In the last column of Table 1, available experimental data are shown as well. It can be seen that accurately reproducing the experimental values is an extremely difficult task (an error of 100 mV corresponds to an error of 9.6 kJ mol^{-1}, which is well within the error bars of the quantum-chemical and solvation methods used for the calculations of the three terms contributing to the total ΔG_{ox}). In practice, a comparison is usually done for a series of chemically similar compounds (using the simplest system as an internal calibration), such as the one reported in our previous work on a series of $[Ru(bipy)_3]^{2+/3+}$ derivatives.[16] Nevertheless, three observations can be derived from the data presented in Table 1.

First, the calculated values depend on the size of the system. The best agreement was obtained for the largest redox couple, $[Ru(bipy)_3]^{2+/3+}$ ($\Delta_{exp/calc} \approx 50$ mV). The agreement was poorer for the smaller $[Ru(en)_3]^{2+/3+}$ and $[Ru(NH_3)_6]^{2+/3+}$ systems ($\Delta_{exp/calc} \approx 246$ and 370 mV, respectively), whereas the largest deviation ($\Delta_{exp/calc} \approx 1$ V) was found for the reference state, $[Ru(H_2O)_6]^{2+/3+}$. Quantum-chemical calculations of $[Ru(H_2O)_n]^{2+/3+}$ reduction potentials were addressed in detail by Cramer and Truhlar,[47] who concluded that inclusion of explicit water molecules in the second solvation shell is necessary to obtain a reduction potential of ∼0.2 V, in agreement with the experiment. To further elaborate on this hypothesis, we demonstrated that (i) the calculated reduction potentials strongly depend on the accuracy of the calculated solvation energies (as pointed out by the above authors) and (ii) the implicit solvation models yield reasonably accurate solvation energies for larger ligands, so it is not necessary to include the explicit second solvation shell into the calculations in those cases. To this end, calculations were carried out for the $[Ru(H_2O)_6]^{2+/3+}\cdot(H_2O)_{12}$, $[Ru(NH_3)_6]^{2+/3+}\cdot(H_2O)_{14}$, and $[Ru(bipy)_3]^{2+/3+}\cdot(H_2O)_{27}$ systems, i.e., for a subset of the studied complexes with k water molecules in the second solvation shell. The equilibrium geometries of these systems can be found in the Supporting Information (together with a detailed description of the protocol used to obtain the starting geometries of the systems), whereas the calculated energies and reduction potentials are listed in Table 1. Indeed, the deviation between the calculated values of E^0 was largest for the $\{[Ru(H_2O)_6]^{2+/3+}/[Ru(H_2O)_6]^{2+/3+}\cdot(H_2O)_{12}\}$ pair (-0.78 V), followed by the $\{[Ru(NH_3)_6]^{2+/3+}/[Ru(NH_3)_6]^{2+/3+}\cdot(H_2O)_{14}\}$ pair (-0.56 V); the difference was very small for the $\{[Ru(bipy)_3]^{2+/3+}/[Ru(bipy)_3]^{2+/3+}\cdot(H_2O)_{27}\}$ pair (0.06 V).

Second, in spite of the fact that only one comparison is available for the formal $(4-) \rightarrow (3-)$ oxidation process (see Table 1), it seems that the reduction potentials for this process were underestimated by ∼0.5 V. We obtained identical systematic errors in our attempts to calculate reduction potentials of ferrocene derivatives attached to a DNA strand or to a nucleotide where the presence of four negative charges on the triphosphate moiety led to a negative shift of 0.5−0.7 V (the experimental data are reported in ref 48, and the computational data are not shown). Both of the above points demonstrate that it is essential to accurately calculate the solvation energy. This goal can be achieved by using several explicit solvent molecules

(46) *CRC Handbook of Chemistry and Physics*, 88th ed.; Lide, D. R., Ed.; CRC Press: Boca Raton, FL, 2007.
(47) Jaque, P.; Marenich, A. V.; Cramer, C. J.; Truhlar, D. G. *J. Phys. Chem. C* **2007**, *111*, 5783−5799.
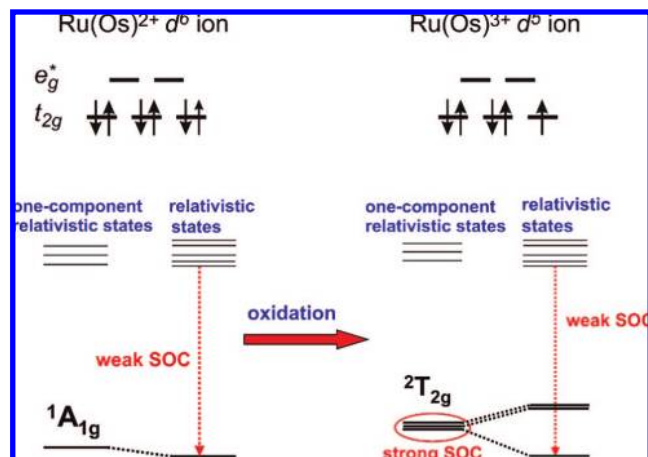
Figure 2. Schematic representation of SOC effects on the values of the reduction potentials of Ru$^{2+/3+}$ and Os$^{2+/3+}$ octahedral complexes. The strong SOC within the degenerate $^2T_{2g}$ state results in extra stabilization of the doublet ground state of the Ru^{3+} and Os^{3+} complexes with respect to the singlet ground state of the Ru^{2+} and Os^{2+} complexes. This causes a negative shift of the reduction potentials.

(as demonstrated above) and/or by using more-advanced solvation models that involve several empirical parameters (e.g., COSMO-RS).[49] However, improvement of the $\Delta\Delta G_{solv}$ term in ΔG_{ox} is not the primary scope of this work.

Third, there was a noticeable deviation in the Os$^{2+/3+}$ reduction potentials, which were apparently overestimated by ~200−400 mV. Since excellent agreement between the calculations and experiments was obtained in our calculations of the analogous ruthenium systems,[16] this discrepancy led us to consider the neglect of SOC as a possible systematic error. The qualitative considerations, which are schematically illustrated in Figure 2, and the respective results from the calculations are discussed in the next section.

Model Structures of the [M(CN)$_6$]$^{4−/3−}$, [MCl$_6$]$^{4−/3−}$, and [M(H$_2$O)$_6$]$^{2+/3+}$ Complexes Attaining O_h or T_h Symmetries. Qualitatively, SOC effects on the values of the reduction potentials of octahedral d^6 ions of the second- and third-row transition metals (i.e., d$^6 \rightarrow$ d^5 processes) can be estimated from the electronic ground-state configurations of the reduced and oxidized forms of the complexes (see Figure 2). It is known that octahedral Ru^{2+} and Os^{2+} complexes have singlet ground states ($^1A_{1g}$),[50] which are not influenced by SOC in the zero-order approximation defined by neglecting all of the excited states (i.e., using essentially the crystal-field model). Their oxidized counterparts, the corresponding Ru^{3+} and Os^{3+} complexes, are expected to have $^2T_{2g}$ ground states (or ^2T_g in T_h symmetry). SOC then splits this sixfold-degenerate state (twofold in the spin variable and threefold spatially) into the Kramers doublet $E_{(5/2)g}$ stabilized by SOC and the fourfold-degenerate $G_{(3/2)g}$ state destabilized by SOC [these states are $E_{(1/2)g}$ and $G_{(3/2)g}$, respectively, in T_h symmetry]. The stabilization of the ground state by SOC is a consequence of the fact that the spin−orbit Hamiltonian is Hermitian and has a purely imaginary spatial part. Hence, its expectation values in states described by real wave functions are both real and purely imaginary and thus equal to zero. As a result, the matrix of the

spin−orbit Hamiltonian in a basis consisting of the real eigenfunctions of the one-component relativistic Hamiltonian has vanishing diagonal elements. Since diagonalization of the matrix does not alter its trace, splitting of a manifold of degenerate one-component relativistic states due to SOC among them always leads to stabilization of the lowest-energy level, while the centroid of the split levels remains unchanged. Moreover, inclusion of higher excited states into the perturbation expansion further decreases the energy of the ground state, E, according to the relation

$$E = E_0 + \langle \Psi_0 | \hat{H}_{SO} | \Psi_0 \rangle + \sum_{i=1}^{\infty} \frac{|\langle \Psi_i | \hat{H}_{SO} | \Psi_0 \rangle|^2}{E_0 - E_i} \qquad (3)$$

where

$$\langle \Psi_0 | \hat{H}_{SO} | \Psi_0 \rangle = 0 \qquad (4)$$

Since the zero-order ground-state energy E_0 is smaller than E_i for all i, the value of E is always smaller than E_0.

To quantify these effects, first-order QDPT calculations with a zero-order space consisting of the three state-averaged CASSCF(5,3) wave functions for the $^2T_{2g}$ ground state were carried out. The results for the [M(CN)$_6$]$^{3−}$, [MCl$_6$]$^{3−}$, and [M(H$_2$O)$_6$]$^{3+}$ complexes are depicted in Figure 3. The [M(H$_2$O)$_6$]$^{3+}$ complex is not strictly octahedral but rather belongs to the point group T_h when the geometrical arrangement of the ligands depicted in Figure 3 is considered. However, the sixfold degeneracy is not lifted in this point group, and thus, all of the conclusions apply for this complex as well.

As discussed qualitatively above, it can be seen that SOC splits the O_h $^2T_{2g}$ [T_h ^2T_g] state into the $E_{(5/2)g}$ [$E_{(1/2)g}$] and $G_{(3/2)g}$ states. The magnitude of the splitting was 1354−1573 cm^{-1} for the Ru(III) complexes and 4155−5061 cm^{-1} for the Os(III) complexes. The stabilization of the ground state was then 0.112−0.130 eV for the Ru(III) systems and 0.343−0.418 eV for the Os(III) systems. Accordingly, the zero-order estimates of the effect of SOC on the reduction potentials of the octahedral Ru(II/III) and Os(II/III) complexes are approximately −120 mV for Ru and −390 mV for Os.

SOC Effects in Nonsymmetrical Ru$^{2+/3+}$ and Os$^{2+/3+}$ Complexes. In order to further elaborate these ideas and bring them closer to the real systems, the analogous approach was adopted in order to calculate the shifts in the reduction potentials in the set of representative Ru$^{2+/3+}$ and Os$^{2+/3+}$ complexes attaining their equilibrium C_1 geometries (see Figures 3 and 4). First-order QDPT calculations with a zero-order space consisting of the three state-averaged CASSCF(5,3) wave functions for the three near-degenerate Kramers doublets originating in the $^2T_{2g}$ ground state were carried out and compared with the one-component relativistic values (having the CASPT2 energies used in the main diagonal of the two-component Hamiltonian matrix). The results are summarized in Table 2. Because of the loss of symmetry, the $^2T_{2g}$ state of the M^{3+} complexes splits into three Kramers doublets even in the one-component relativistic calculations. The lowest-energy doublet is further stabilized by SOC (see eqs 3 and 4 above).

For most of the complexes, the negative shifts in the reduction potentials correspond to the shifts calculated for the octahedral

(48) Brázdilová, P.; Vrábel, M.; Pohl, R.; Pivoňková, H.; Havran, L.; Hocek, M.; Fojta, M. *Chem.—Eur. J.* **2007**, *13*, 9527−9533.

(49) Klamt, A. *J. Phys. Chem.* **1995**, *99*, 2224−2235.

(50) Cotton, F. A.; Wilkinson, G. *Advanced Inorganic Chemistry*, 4th ed.; Wiley: New York, 1980.

(51) (a) Bernhard, P.; Burgi, H.-B.; Hauser, J.; Lehmann, H.; Ludi, A. *Inorg. Chem.* **1982**, *21*, 3936−3941. (b) Biner, M.; Burgi, H.-B.; Ludi, A.; Rohr, C. *J. Am. Chem. Soc.* **1992**, *114*, 5197−5203. (c) Otsuka, T.; Takahashi, N.; Fujigasaki, N.; Sekine, A.; Ohashi, Y.; Kaizu, Y. *Inorg. Chem.* **1999**, *38*, 1340−1347.
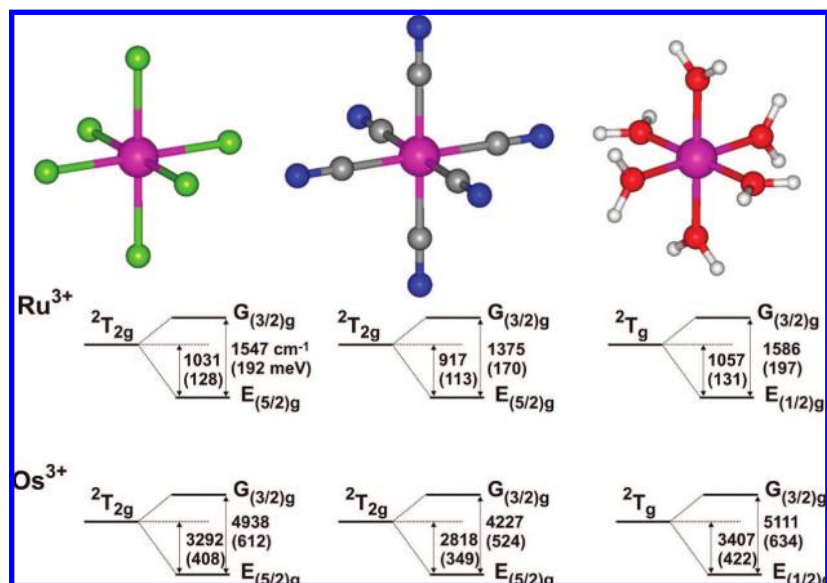
Figure 3. Structures of the octahedral $[M(CN)_6]^{4-/3-}$, $[MCl_6]^{4-/3-}$, and $[M(H_2O)_6]^{2+/3+}$ complexes obtained from the DFT/def2-SVP (including ECPs for Ru and Os) constrained geometry optimization. The splitting of the O_h $^2T_{2g}$ $[T_h$ $^2T_g]$ degenerate state into the $E_{(5/2)g}$ $[E_{(1/2)g}]$ and $G_{(3/2)g}$ states, calculated using the CASSCF(5,3)/CASPT2/CASSI method and the TZP/DZP basis set, is depicted as well. The metal–ligand distances are 2.07, 2.46, and 2.04 Å (2.09, 2.49, and 2.06 Å) for Ru–C, Ru–Cl, and Ru–O (Os–C, Os–Cl, and Os–O), respectively.

complexes. They are slightly smaller, which is a consequence of the symmetry splitting of the one-component relativistic states (the magnitude of the SOC between two states is inversely proportional to the difference in the energies of these states; see eq 3 above). This effect is most pronounced for the hexahydrates of $Ru^{2+/3+}$ and $Os^{2+/3+}$, which have the largest symmetry splitting (~5000 cm^{-1}), resulting in the smallest values of SOC stabilization of the ground states of the oxidized forms.

In our zero-order approximation, SOC has no effect on the ground-state electronic structure of the reduced (singlet) form of the ruthenium/osmium complexes. This approximation is based on the assumption that the lowest-energy triplet states of M^{2+}, which arise from excitations from the highest occupied metal t_{2g} or t_g MOs to the metal e_g^* MOs (assuming the ideal O_h or T_h symmetry, respectively), lie sufficiently high in energy. Analogously, it is believed that SOC of the doublet ground state of M^{3+} with the higher excited states (doublets, quartets, sextets) is less significant because of the large energy gap between the t_{2g} (or t_g) and e_g^* MOs. However, the typical situation is more complicated. For example, the deep colors of $[Ru(bipy)_3]^{2+/3+}$ (red) and $[Os(bipy)_3]^{2+/3+}$ (dark-green to black) indicate that there are some ligand MOs that lie between the metal t_{2g} (or t_g) and e_g^* orbitals. Nevertheless, we can still consider the zero-order model as appropriate for the given purpose, for at least three reasons. First, SOC among the three near-degenerate doublets arising from the distribution of five electrons in the three t_{2g} (or t_g) orbitals is always strong. Second, SOC between the singlet or doublet ground states of the studied complexes and the higher excited states arising from excitations of an electron from the metal t_{2g} (or t_g) orbital to any of the ligand MOs [possibly lying in the gap between the t_{2g} (or t_g) and e_g^* orbitals] should be small, as it typically relies on tiny two-center spin–orbit integrals and only minor contributions from one-center spin–orbit integrals. Third, even if the influence of higher excited states is larger than expected on the basis of the two previous arguments, there is a reasonable chance that the resulting stabilizations of the ground states are nearly the same in both the oxidized and reduced forms of the studied complexes, and thus, these stabilizations will likely compensate for each
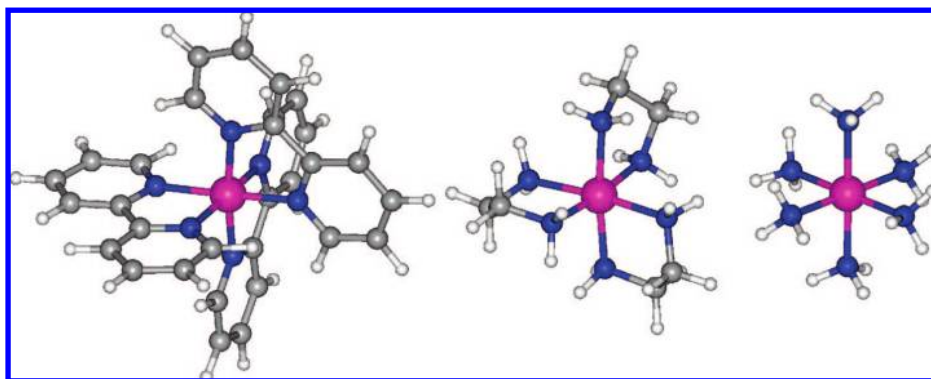

Figure 4. Equilibrium structures of the $[M(bipy)_3]^{2+/3+}$, $[M(en)_3]^{2+/3+}$, and $[M(NH_3)_6]^{2+/3+}$ complexes obtained from the DFT/def2-SVP (including ECPs for Ru and Os) optimizations. The metal–ligand distances are ~2.06, 2.14, and 2.13 Å for Ru^{2+}–N_{bipy}, Ru^{2+}–N_{en}, and Ru^{2+}–N_{NH_3} (2.08, 2.16, and 2.15 Å for Os^{2+}), compared to 2.07, 2.12, and 2.11 Å for Ru^{3+}–N_{bipy}, Ru^{3+}–N_{en}, and Ru^{3+}–N_{NH_3} (2.09, 2.15, and 2.14 Å for Os^{3+}). The calculated equilibrium distances are in very good agreement with the experimental values (an average deviation of 0.01–0.03 Å).[51]

Table 2. Calculated One-Component Relativistic (without SOC) and Two-Component Relativistic (with SOC) Energy Splittings of the Ideally Degenerate $^2T_{2g}$ State into Three Kramers Doublets, Obtained Using the CASSCF(5,3)/CASPT2/CASSI Method and the TZP/DZP Basis Set[a]

complex	2^2A	3^2A	$2E_{1/2}$	$3E_{1/2}$	ΔE^0
$[Ru(H_2O)_6]^{2+/3+}$	3996	5131	4068	5485	−18
$[RuCl_6]^{4-/3-}$	92	214	1500	1613	−116
$[Ru(NH_3)_6]^{2+/3+}$	407	487	1467	1712	−94
$[Ru(en)_3]^{2+/3+}$	1284	1326	1770	2186	−56
$[Ru(bipy)_3]^{2+/3+}$	1821	1829	2120	2547	−42
$[Ru(CN)_6]^{4-/3-}$	286	296	1336	1474	−92
$[Os(H_2O)_6]^{2+/3+}$	4756	6324	6139	8591	−151
$[OsCl_6]^{4-/3-}$	202	272	4863	4970	−387
$[Os(NH_3)_6]^{2+/3+}$	610[b]	638	4862	5125	−362
$[Os(en)_3]^{2+/3+}$	1721	1858	4975	5391	−280
$[Os(bipy)_3]^{2+/3+}$	2265[b]	2281	5138	5445	−250
$[Os(CN)_6]^{4-/3-}$	293[b]	305	4286	4367	−333

[a] Excitation energies (columns 2−5) are in cm^{-1}. The reference energy (0 cm^{-1}) for the values in columns 2 and 3 is the energy of the relativistic ground state (1^2A) for the one-component relativistic calculations, and that for the values in columns 4 and 5 is the energy of the relativistic ground state ($1E_{1/2}$, where $E_{1/2} = B_{1/2} \oplus B_{1/2}$ stands for the reducible representation of the double group C_1^2) for the two-component relativistic calculations. The energy difference ΔE^0 (in mV) between the two ground states (1^2A and $1E_{1/2}$) is then shown in column 6; it corresponds to the shift in the reduction potential due to SOC. [b] CASSCF(5,3)/CASPT2/CASSI/TZP/DZ values.

other. In the next section, these qualitative arguments are addressed quantitatively.

Contribution of Higher Excited States to the Stabilization of the Singlet and Doublet Ground States Due to SOC. In order to estimate the effect of higher excited states that may contribute to the stabilization of the ground state, it is essential to consider both the SOC matrix elements and the energy differences between the interacting states: the SOC stabilization is proportional to the square of the SOC matrix elements and inversely proportional to the energy differences. To this end, a series of MRCI calculations were carried out for the model complexes $[M(NH_3)_6]^{2+/3+}$, $[M(H_2O)_6]^{2+/3+}$, and $[M(CN)_6]^{4-/3-}$. Subsequent first-order QDPT calculations with the one-electron mean-field spin−orbit Hamiltonian taken from the perturbation to the one-component relativistic Hamiltonian yielded estimates of the influence of higher excited states on the stabilization of the 1^1A_{1g} and 1^2T_{2g} (1^1A and 1^2A in the case of nonsymmetrical systems) states as a result of SOC.

Table 3 summarizes the calculated values of the stabilization of the singlet ground state by all of the considered excited states and that of the lowest-energy doublet state by the D_2 and D_3 states only and by all of the considered excited states; the numbers of states taken into account to interact with both of the ground states are also included. A more detailed examination is presented in Tables S3 and S4 in the Supporting Information. There, it is demonstrated that the stabilization of the singlet and doublet ground states is essentially converged with respect to the number of interacting states and that an identical picture is obtained from MRCI-based QDPT calculations using natural orbitals as the MO basis. Therefore, these supplementary calculations essentially confirm the overall picture that can be obtained from Table 3.

Two observations can be made on the basis of the values presented in Table 3. First, the stabilization of the ground doublet by the D_2 and D_3 states is usually the dominant contribution to the overall stabilization. Second, and more importantly, the difference between the S_0 and D_1 stabilizations due to higher excited states is 3−95 cm^{-1} for the studied Ru$^{2+/3+}$ complexes

Table 3. Calculated Values of the Stabilization of the Singlet Ground State (1^1A) by SOC with Higher Excited States of Various Spin Multiplicities and the Stabilization of the Lowest-Energy Doublet State (1^2A) by SOC with only the 2^2A ($=D_2$) and 3^2A ($=D_3$) states (the Near-Degenerate Counterparts of 1^2A) and with Higher Excited States[a]

complex	ΔE_{stab} (cm^{-1})[b]				Δ_{SD} (mV)[f]
	1^1A ($=S_0$)[c]	1^2A ($=D_1$)[c]			
	S_{1-15}, T_{1-10}, 5_{1-5}[d]	D_2, D_3[d]	D_{2-15}, Q_{1-10}, 6_1[d]	D_{4-15}, Q_{1-10}, 6_1[d,e]	
$[Ru(NH_3)_6]^{2+/3+}$	−219	−449	−692	−243	3
$[Ru(H_2O)_6]^{2+/3+}$	−372	−170	−545	−375	0.3
$[Ru(CN)_6]^{4-/3-}$	−41	−799	−935	−136	12
$[Os(NH_3)_6]^{2+/3+}$	−1629	−3399	−5277	−1878	31
$[Os(H_2O)_6]^{2+/3+}$	−2686	−1539	−4427	−2888	25
$[Os(CN)_6]^{4-/3-}$	−110	−2476	−2737	−261	19

[a] The CAS(5,5)/MRCI/TZV-DKH method for M^{3+} ions [CAS(6,5)/MRCI/TZV-DKH for M^{2+} ions] was applied, using the computational protocol described in Computational Methods. [b] ΔE_{stab} is the stabilization energy of state X due to SOC: $\Delta E_{stab} = E_{rel-SOC}(X) - E_{non-rel}(X)$. [c] Ground state; the notation for one-component relativistic states has been used. [d] Interacting states, denoted as follows: singlets (S), doublets (D), triplets (T), quartets (Q), quintets (5), and sextets (6). [e] Stabilization of D_1 by all but the two near-degenerate excited states D_2 and D_3. [f] Δ_{SD} is the difference between the stabilization of S_0 from all of the excited states and that of D_1 from all but the two near-degenerate excited states D_2 and D_3: $\Delta_{SD} = \Delta E_{stab}(S_0;$ all states$) - [\Delta E_{stab}(D_1; D_2, D_3$ only$) - \Delta E_{stab}(D_1;$ all states$)]$. Positive values indicate that D_1 is stabilized to a greater extent than S_0 by the interaction with higher-energy states.

and 151−248 cm^{-1} for the Os$^{2+/3+}$ complexes. Therefore, it seems that neglecting these effects may introduce errors of ∼10 mV in the reduction potentials of Ru complexes and ∼30 mV for Os complexes. In both cases, this accounts for ∼10% of the overall SOC effect on the value of the reduction potentials. This supports the idea that the first estimates of the effect of SOC on the values of the Ru$^{2+/3+}$ and Os$^{2+/3+}$ reduction potentials (as provided by the CASPT2/CASSI-based QDPT calculation with minimum active space) are sufficiently accurate.

Conclusions

In this work, we have shown that the SOC splitting of the $^2T_{2g}$ state (in ideal O_h symmetry) into the $E_{(5/2)g}$ doublet and $G_{(3/2)g}$ quartet states shifts the values of the reduction potentials of octahedral ruthenium and osmium complexes by ΔE^0(Ru) $\approx$ −120 mV and ΔE^0(Os) $\approx$ −390 mV (or by −70 and −300 mV, respectively, in the case of symmetry-perturbed systems). We have also shown that the stabilization of the oxidized form originating from this splitting of its $^2T_{2g}$ ground state should play a decisive role in shifting of the values of the reduction potentials by SOC, as the contribution from higher excited states is believed to be smaller and, importantly, of approximately the same magnitude for both the reduced and oxidized forms. Last but not least, we have demonstrated that accurate predictions of reduction potentials must allow for an accurate treatment of solvation energies, especially in the case of smaller ligands, such as water or ammonia; such a treatment involves explicit inclusion of the second solvation shell. However, it seems that the solvation effects are adequately described by PCM-like (or implicit solvation) models in the case of larger ligands, for which the calculated (and SOC-corrected) values of the reduction potentials were in a good agreement with the experimental values. This demonstrates that accurate predictions of reduction potentials for the Ru$^{2+/3+}$ and especially the Os$^{2+/3+}$ redox couples must allow for the effect of SOC, since its neglect leads to the aforementioned systematic error in the calculated values.

Supporting Information Available: Equilibrium geometries and molecular energies of all the studied molecules (for all of the methods used) and tables describing the basis-set dependence of the calculated CASSCF(5,3)/CASPT2/CASSI energy splittings and the convergence of MRCI values with the number of excited states. This material is available free of charge via the Internet at http://pubs.acs.org.

JA800616S